PRAMANA
— journal of
physics

Supplement to Vol. 41
December 1993
pp. 183–195

Recent results from CDF

NABA K MONDAL
Tata Institute of Fundamental Research, Bombay 400005, India

1. Detector Status

The CDF detector in its original form consists of a 2000 ton central detector and is made up of solenoidal magnet, steel yoke, tracking chambers, electromagnetic and hadronic shower counters, muon counters and a pair of forward-backward detectors consisting of segmented TOF counters, e.m. & hadronic shower counters and muon toroidal spectrometers [1]. A perspective view of the original CDF detector is shown in Fig. 1. This detector was in operation during 87-88 and the total collected

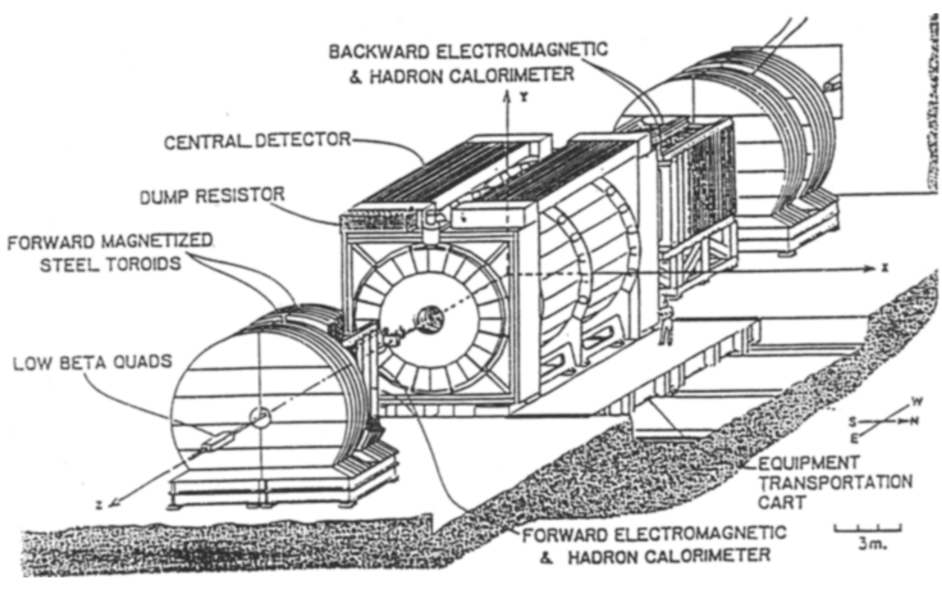

Figure 1. Perspective view of the original CDF detector.

integrated luminosity on tape during this period was about 4.3 pb^{-1}.

During the collider shutdown (89-92), CDF has made some detector improvement [2]. Two new muon systems have been added. The first one upgrades the existing central muon system with additional steel of about 2 interaction lengths. This will reduce the hadronic punch-through by an additional factor of 10. The second muon upgrade extends the coverage of central muon system from $|\eta| = 0.63$ to 0.9. A new silicon vertex detector has also been installed around the interaction point. It consists of two barrels, each with 4 layers of silicon strip detectors. The expected impact parameter resolution of this detector is about 13 μm for $p_t > 10$ GeV and is well suited for detecting secondary vertices from b hadron decay. A new central preshower detector has been installed. This will improve electron identification and also reduce systematic uncertainties on the prompt photon cross section.

2. Physics status

2.1. Top search

At $\sqrt{s} = 1.8$ TeV, the dominant process for top production is $p\overline{p} \rightarrow t\overline{t}$. In the Standard Model, top is expected to decay via "weak charged current" to $t \rightarrow wb$. During 1988-89 Tevatron run CDF has collected 4.1 pb^{-1} of data and has established a lower limit on m_{top} of 91 GeV at 95% C.L. (see Fig. 2) for Standard Model charged current decay of the top quark [3]. On the other hand, the measured masses of W

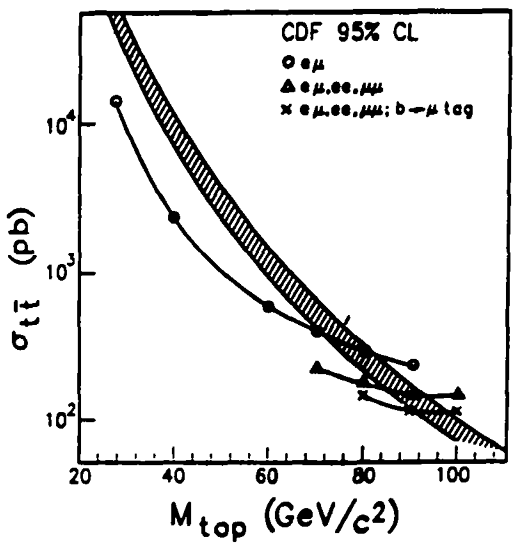

Figure 2. The 95% CL limits on $\sigma_{t\overline{t}}$ compared with a band of theoretical predictions from Standard Model.

and Z bosons, weak neutral current data and precision measurements of charge asymmetries in Z decay suggest that top mass is probably less than 200 GeV. Thus within the framework of Standard Model the mass of the top quark lies between 91 and 200 GeV. The expected integrated luminosities from Run 1A (ongoing) and Run 1B (Schedule for 92-93) are 25 pb^{-1} and 100 pb^{-1} respectively. Following the commissioning of the main injector in 96-97, the expected integrated luminosity is as high as 1 fb^{-1}. The prospect of discovering the top quark at Tevatron in next few years is therefore very bright.

2.1.1. Top decay signature

At the tevatron energy the top quark will be pair-produced by $q\bar{q}$ and gg fusion. In the minimal Standard Model, there is only one t-quark decay mode: $t \rightarrow Wb$. Now depending upon whether each of the intermediate decay components ($W\bar{W}$ $b\bar{b}$) having a hadronic or a semi-leptonic decay, three different types of event topologies are expected.

(i) **All Jets :** Here both W decay into quarks. Although this channel has about 44% branching ratio, it also has large QCD background. even though the statistics will be largest, it will be difficult to establish the existence of the top quark through this channel due to large QCD background.

(ii) **Lepton + jets:** Here one W decay into leptons (either e or μ) the other W decay into quarks. This channel has a total of 30% branching ratio. The signature for this mode is a high transverse momentum lepton (e or μ), high missing energy and a few jets including two b-jets. There are however, significant background for this channel from QCD W + multijet production. Since the background events are not expected to have any b-quark in general, b-tagging will help in identifying lepton + jet events from $t\bar{t}$ and in reducing the W + jet background. In the upgraded CDF detector, b's can be tagged either from the presence of a secondary vertex, or by identifying soft leptons from the semileptonic b-decays [2]. Table 1 below gives the expected number of top events and W + jet background events in 25 pb^{-1} of data.

Table 1

	cross section pb	High P_T l + SVX b tag	High P_T l + soft l
top 120	35.3	13	14
top 140	15.6	9	9
top 160	7.7	5	
W + jets		~ 1	~ 4

(iii) **Dileptons:** In this mode both the W's decay into leptons (e or μ). The signature for this mode is two isolated high P_T leptons (e or μ) and missing transverse energy. The total branching ratio for this mode is 5%. This does not include dileptons from $t \rightarrow \tau \rightarrow e$ *or* μ decays, which contributes to about 10% of the dilepton signal. Top search through high P_T dilepton channels has many advantages. This is one of the cleanest channels to establish top decay, since the background here is extremely low and can be rejected with topology cuts. With enhanced B-tagging ability using the Silicon microvertex detector for the ongoing run, the top detection efficiency through this channel will be even higher. Table 2 below gives the number of expected high

P_T dilepton events from $t\bar{t}$ decay after taking into account CDF detection efficiency [2].

Table 2

top mass	predicted cross section	expected events for 25 pb^{-1}
100 GeV	91 pb	13
120 GeV	36 pb	7.2
140 GeV	16 pb	3.2
160 GeV	7.7 pb	1.5

2.2. Testing QCD with jets:

To test QCD with jets, CDF has studied jet shape, inclusive jet cross section etc [4]. More recently, CDF has also studied four jet events in order to look for double parton scattering [5].

2.2.1. Jet cross section and jet shape

Experimentally jets are defined as the energy inside a cone of radius R $= \left((\Delta\eta)^2 + (\Delta\phi)^2\right)^{\frac{1}{2}}$. The value of R used by CDF group is 0.7. CDF measure E_T = ESinθ, and correct the E_T spectrum for calorimeter response, underlying event energy inside the jet cone and energy resolution smearing of the spectrum. The NLO (Next to Leading Order) QCD calculation also uses a similar definition in which the two partons are merged if they fall inside the same cone. The plot in Fig. 3 shows the cross section dependence on the cone radius R. It is clear from this Figure that the data have a behaviour similar to QCD, with a steeper dependence on the cone size then what NLO calculation predicts. This may be due to the non-inclusion of still higher order terms. However, α_s^3 calculation appears to be able to qualitatively reproduces the effect. The comparison of the jet shape with the prediction of the α_s^3 calculation shows that the addition of an extra parton in the final state explain the jet shape much better. CDF has also measured the p_T flow around the jet axis for jets of transverse energy 100 GeV. It has defined a *shape*(r) function by measuring the p_T fraction inside a cone of radius r, smaller than the jet cone size R_0. This function is normalised to be equal to 1 for r=R_0 and goes to zero for r $\to$ 0. The axis of the jet is defined by the calorimeter using cone algorithm with cone radius R_0=1. Jets were selected in the central rapidity region $0.1 < |\eta| < 0.7$, and with transverse energy in the range $95 < E_T < 120$ GeV. Fig. 4 shows both data and theory based on NLO QCD calculation. The agreement is reasonably good indicating that the existence of an extra parton in the final state can give a good description of the jet shape.

2.2.2. Inclusive jet cross section:

Inclusive jet cross section can be used as a test of QCD and allows us to make tighter constrain of parton distribution functions (PDFs). This is specially true

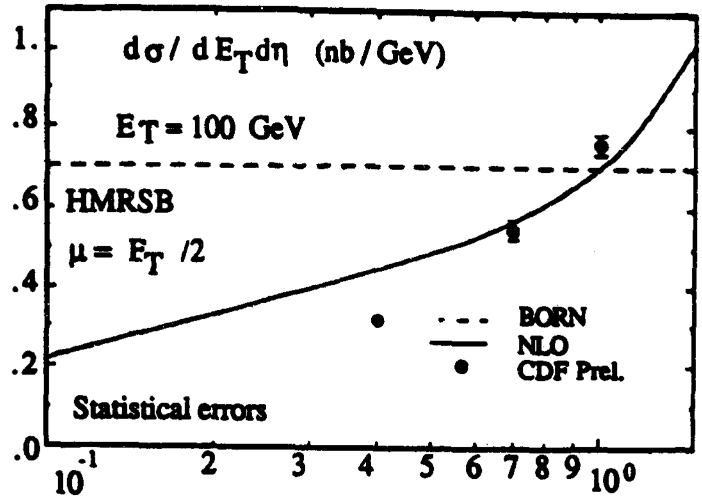

Figure 3. Jet cross section as a function of cone radius R.

if we use next-to leading-order calculations (NLO) of jet production as it is less sensitive to the choice of renormalization scale then leading-order (LO). One can also use the p_T distribution to look for quark compositeness, which will be a signal for new physics beyond the Standard Model. If quarks are composite particles, a contact term of unit strength between left handed quarks will be added to the Lagrangian [6] for interactions at energies less than the compositeness energy scale Λ_c. This contact term being independent of p_T will dominate over the normal QCD term which decreases as $1/p_T^4$, and will produce excess of high p_T jets which will be a signal for quark compositeness. The CDF measurement of the inclusive jet cross section is shown in Fig. 5a, in comparison to NLO QCD prediction plus composite quarks. The data does not show any statistically significant contribution due to the contact term and set the limit $\Lambda_c > 1.4$ TeV at 95% confidence level. The corresponding compton wavelength is $< 1.4 \text{ X } 10^{-17}$cm. Fig. 5b shows the comparison of CDF data to NLO QCD calculations with different PDFs [7]. The data is in better agreement with all PDFs except HMRS set E.

2.2.3. Four jet events

Although the dominant production mechanism for events containing four high p_T jets at the Tevatron collider is double gluon bremsstrahlung (DB), they can in principle be produced by double parton scattering (DP). by comparing the kinematic properties of four-jet events in $p\overline{p}$ collisions CDF has placed an upper limit on the double parton scattering crosssection [5]. They have performed a statistical search for DP interactions using two variables. The first variable, S, minimize the p_T imbalance of jet pairs and is defined in the following way:

$$S(1+2+3+4) \equiv \sqrt{\left[\left(\frac{|\vec{p}_{T_1}+\vec{p}_{T_2}|}{\sqrt{p_{T_1}+p_{T_2}}}\right)^2+\left(\frac{|\vec{p}_{T_3}+\vec{p}_{T_4}|}{\sqrt{p_{T_3}+p_{T_4}}}\right)^2\right]/2}. \qquad (1)$$

The second variable, Δ_s is defined using the angles between jets. If ϕ_{ij} is the azimuthal angle of the vector formed with jets i and j, then $\Delta_s = \phi_{ij} - \phi_{kl}$, where

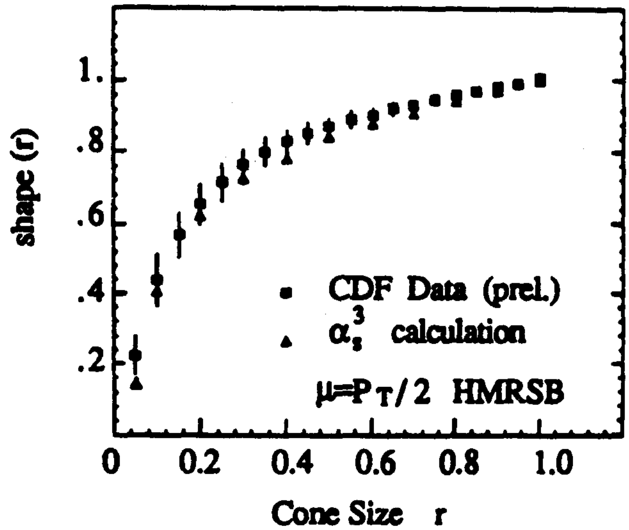

Figure 4. Jet shape - Data versus NLO Theory.

ij and kl pairing of jets is the result of the minimization of the variable S described above.

A fit to the CDF data using an admixture of DP and DB shapes results in a 16% DP signal for Δ_s, but only 2% signal for S. This is shown in Fig. 6a. The difference is attributed due to the presence of a fifth jet in the data. By introducing a cut on the p_T of 5th jet, CDF observed that both results converges for $p_{T5} < 13$ GeV/c. This is shown in Fig. 6b. Corresponding value for $N_{DP}/N_{DB} = 0.051 \pm 0.013$ (stat). Their preliminary determination of systematic uncertainties yields $\sigma_{DP} = 68 \pm 28$ nb. Using this, CDF put a limit $\sigma_{DP} < 120$ nb at 95% C.L.

2.2.4. Isolated double prompt photon production

By studying isolated double photon production, one can probe the gluon distribution and test QCD. In addition, production of two photons is an important background to Higgs $\rightarrow \gamma\gamma$ at the SSC/LHC. We need to understand this background. Also $\gamma\gamma$ system is ideal for measuring initial state transverse momentum. The three types of processes that contribute to the two photon cross sections are shown in Fig. 7. These are Born diagram (qq $\rightarrow \gamma\gamma$), box diagram (gg $\rightarrow \gamma\gamma$), and diagram with photon bremsstrahlung. CDF has used the following triggers for double photon detection; (a) two clusters of electromagnetic energy, each with $E_T > 10$ GeV and HAD/EM $< .125$. Within the P_T range of 10 to 35 GeV, there are 149 diphoton candidates (298 photons). In Fig. 8 we show the diphoton cross section measured by CDF as a function of P_T of the photon [8], each photon has been entered separately in this plot. This observed di-photon cross section is compared to NLO QCD and leading order QCD. It is clear from this plot that the measured di-photon cross section by CDF is significantly above the QCD prediction.

2.3. Exotic particle search

CDF has searched for a number of exotic particles that can be directly produced in $p\overline{p}$ collisions [9]. Table 3 below is a partial list of such particles and the corre-

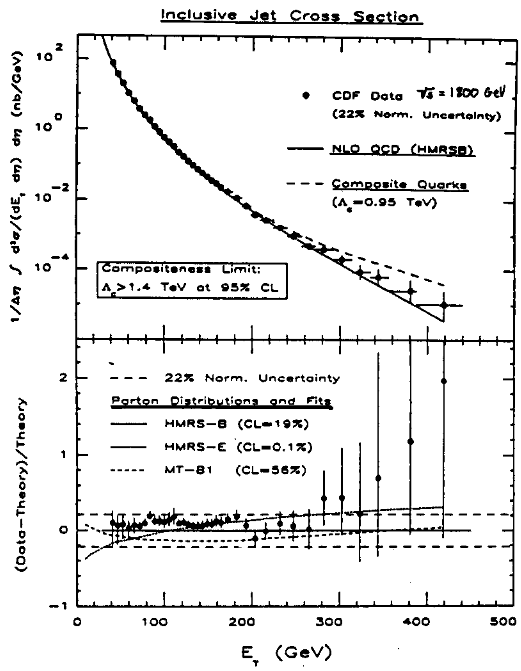

Figure 5. The inclusive jet cross section vs. E_T compared with (a) NLO QCD plus compositeness and (b) NLO QCD with a variety of parton distribution functions.

sponding example theory which predict their existence.

2.3.1. W' limit

CDF has searched for $p\bar{p} \rightarrow W' \rightarrow e\nu$ or $\mu\nu$ events The signal for W' will be similar to that of a ordinary W i.e. a peak in the transverse mass ${M_T}^{l\nu}$ distribution. CDF has searched for such additional peak in $M_T > M_W$. The expected M_T distribution resulting from the ordinary W and an additional W' is calculated using MC technique. The highest M_T events observed are at 185 GeV (electron) and 205 GeV(muon). To search for the W', a maximum likelihood fit of the data to the W plus W' transverse mass distribution is made. The 95% confidence level limit on σ.B as a function of transverse mass is shown in Fig. 9. σ.B for a W' with Standard Model coupling is also shown in this Figure. CDF data suggest that for a W' with Standard Model coupling,

$$M_{W'} > 520\, GeV/c^2 \text{ (at 95\% CL).}$$

2.3.2. Z' limit

CDF has searched for $p\bar{p} \rightarrow Z' \rightarrow ee \text{ or } \mu\mu$ events. The measured lepton pair mass distribution is shown in Fig. 10. It is in excellent agreement with the Monte Carlo prediction for Drell-Yan production of dileptons from Z^0 decay and from virtual photon γ^* decay. The 95% CL limits on $\sigma(Z').B_{ll}$ as a function of Z' mass is shown in Fig. 11. Also shown in the same Figure is the predicted $\sigma.B_{ll}$ for a Z' with Standard Model coupling. CDF data suggest a lower limit on the Z' mass,

$$M_{Z'} > 412\, GeV/c^2 \text{ (at 95\% CL).}$$

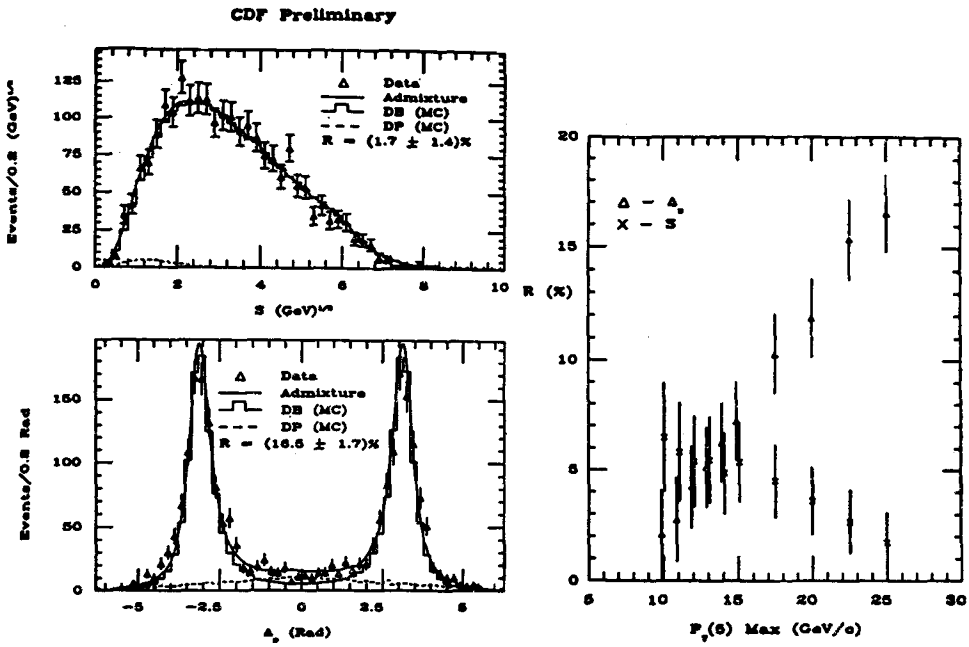

Figure 6. (a) Four-jet data fitted to an admixture of DB and DP shapes using S and Δ_s, (b) Fraction R for S and Δ_s versus maximum allowed p_{T5}.

2.3.3. l.q compositeness

If leptons and quarks are composite particles with common constituents, then there will an effective lepton-quark contact interaction [10] which will cause a flattening of the dilepton mass distribution at high mass. Based on the absence of e^+e^- events with $M_{ll} > 200$ GeV, CDF puts limits on the scale of such an effective contact interaction (see Fig. 12). CDF data indicate that $\Lambda^-_{LL} > 2.2$ TeV and $\Lambda^+_{LL} > 1.7$ TeV at 95% CL, where the scale Λ corresponds to a left-left electron-quark coupling, and the -(+) sign corresponds to constructive (destructive) interference with the dominant u quark contribution. The corresponding limits on a muon-quark compositeness scale are $\Lambda^-_{LL} > 1.6$ TeV and $\Lambda^+_{LL} > 1.4$ TeV at 95% CL.

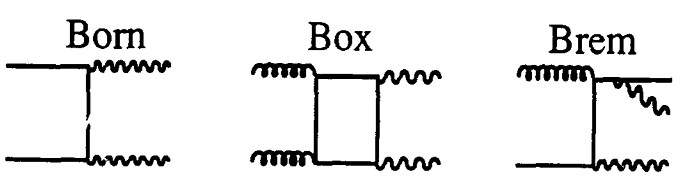

Figure 7. Processes contributing to the two photon cross section.

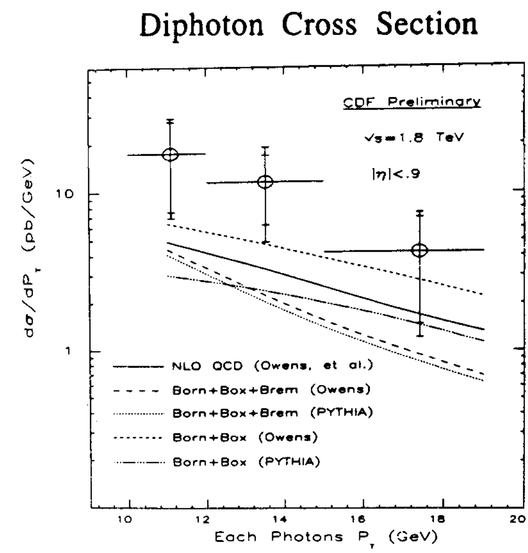

Figure 8. The isolated double prompt photon cross section compared to QCD predictions.

2.3.4. Leptoquark search

Recently CDF has presented its result on the search for generation-1 leptoquarks, LQ_1 [11]. Leptoquarks are expected to be pair produced via gg and $q\bar{q}$ annihilation. The leptoquarks are assumed to decay rapidly to first generation leptons and quarks. Assuming Q(LQ_1) = -1/3e leads to the following possible decays.

$$LQ_1 \rightarrow u + e^- \qquad (\mathrm{BR = x}),$$
$$LQ_1 \rightarrow d + \nu_e \qquad (\mathrm{BR = 1 - x}).$$

CDF has searched for LQ_1 pairs in two channels. In the case where both leptoquarks decay to ue, the expected signature will e^+e^- + two jets with rate x^2. In the (ue)

Table 3

Exotic Particle	Example Theory
W'	LR Sym. models (W_R, ν_R, Z_R)
Z'	$E_6 \rightarrow SU(5)\ X\ U_\chi(1)\ U_\phi$
l.q compositeness	l,q share constituents
leptoquark	E_6 exotic color 3 (B = $\frac{1}{3}$, L=1)
$\tilde{q}$, $\tilde{g}$	SUSY

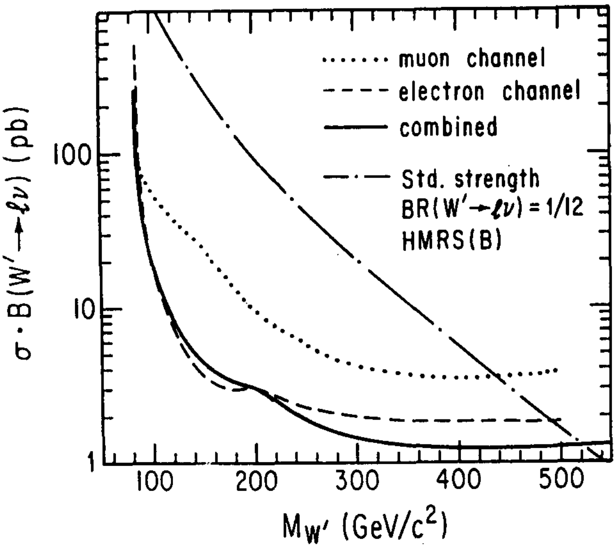

Figure 9. The 95% C.L. limits on $\sigma(W').B_{ll}$ for $W' \rightarrow \mu\nu(dots)$, $W' \rightarrow e\nu$ (dashes) and combined.

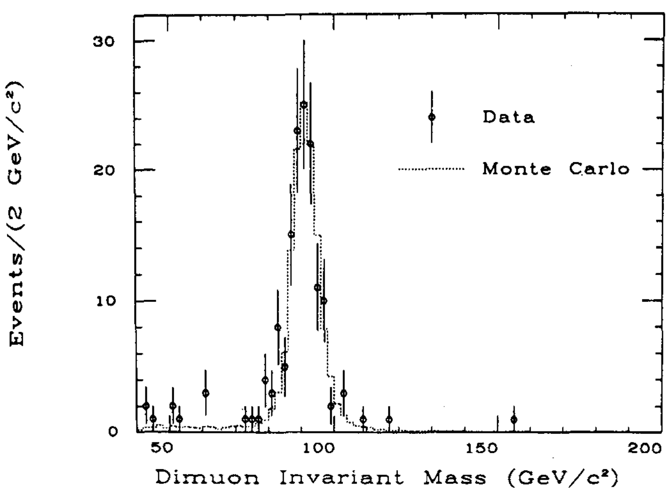

Figure 10. The invarient mass distribution for oppositely charged dimuon candidates.

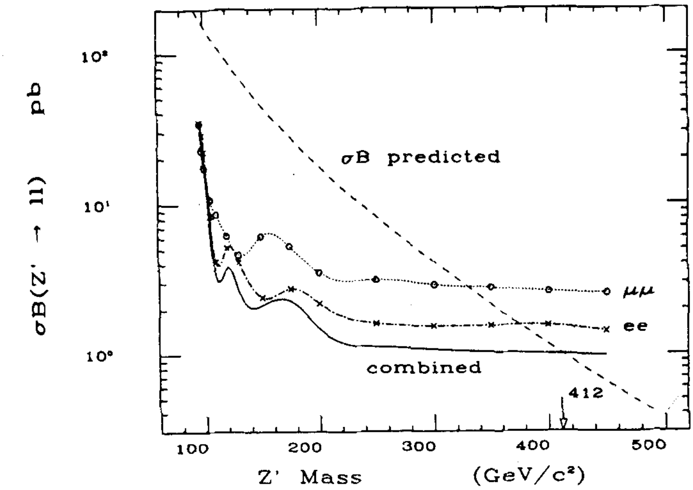

Figure 11. The 95% C.L. limit on $\sigma(Z').B_{ll}$ for Z' production from the dimuon (dotted line), dielectron (dashed-dotted line), and combined channels (solid line).

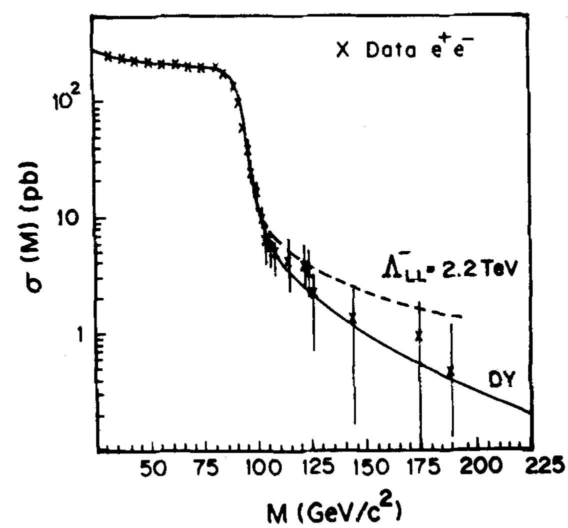

Figure 12. Integrated cross section for electron pair productions. DY prediction (solid) and curves for Λ_{ll}^{-} at 95% CL is also shown.

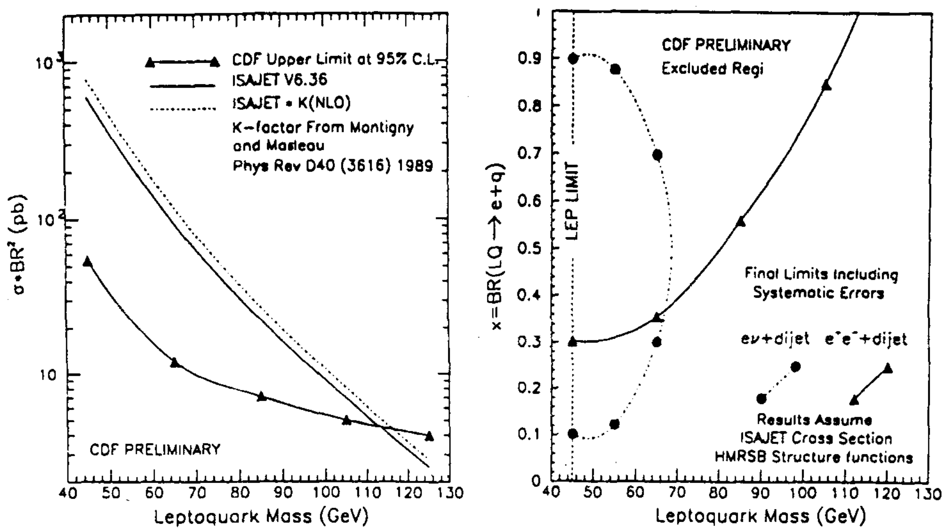

Figure 13. (a) Limits on $\sigma.x^2$ at 95% CL. (b) Excluded x vs M_{LQ} at 95% CL.

$(d\nu_e)$ channel, the signature will be $e^{\pm}\nu_e$ + two jets and the corresponding rate will be 2x(1-x). In the absence of a positive signal, and assuming the ISAJET cross section (Fig. 13a), CDF has derived a 95% CL limit on M_{LQ} as a function of charged lepton BR x. The results for both decay channels are shown in Fig. 13b. Data exclude first-generation leptoquarks with masses $M(LQ_1) > 113$ GeV at the 95% CL.

Acknowledgements

This review draws extensively from the presentations by CDF group members at the XXVI ICHEP at Dallas in August 1992 and also at the DPF meeting at Fermi Lab, Batavia in November 1992. Thanks go to all these CDF speakers. I am, however, responsible for mistakes and omissions.

References

[1] F. Abe et al., CDF Collaboration, Nucl. Inst. and Meth. **A271** (1988) 387.

[2] A. Yagil, CDF Collaboration, Talk presented at the DPF meeting, Fermi Lab, U.S.A., November 1992.

[3] F. Abe et al., CDF Collaboration, Phys. Rev. Lett **68** (1992) 447.

[4] B. Flaugher, CDF Collaboration, Talk presented at the XXVI ICHEP, Dallas, August 1992;
F. Abe et al., CDF Collaboration, Phys. Rev. Lett. **68** (1992) 1104.

[5] L.J.Keeble, CDF Collaboration, Talk presented at the DPF meeting, Fermi Lab, U.S.A., November 1992.

[6] E. Eichten, K. Lane, M. Peskin Phys. Rev. Lett **50** (1983) 811.

[7] P. Harriman, A. Martin, R. Roberts, W. Stirling, Phys. Rev. **D42** (1990) 798; Phys. Lett. **B243** (1990) 421;
J. Morfin & W.Tung Z. Phys. **C52** (1991) 13.

[8] R.M.Harris, CDF Collaboration, Talk presented at the DPF meeting, Fermi Lab, U.S.A., November 1992.

[9] M. S. Gold, CDF Collaboration, Talk presented at the XXVI ICHEP, Dallas, August 1992;
F.Abe et al., CDF Collaboration, Phys. Rev. Lett. **68** (1992) 1104.

[10] E. Eichten, K. Lane & M. Peshkin, Phys. Rev. Lett. **50** (1983) 811; E. Eichten FERMILAB PUB-85/178-T.

[11] S.M. Moulding, CDF Collaboration, Talk presented at the DPF meeting, Fermi Lab, U.S.A., November 1992.